

Low-energy optical transitions in intercalated graphite

C. C. Shieh, R. L. Schmidt, and J. E. Fischer

*Moore School of Electrical Engineering and Laboratory for Research on the Structure of Matter,
University of Pennsylvania, Philadelphia, Pennsylvania 19104*

(Received 20 November 1978; revised manuscript received 24 May 1979)

Interband transitions characteristic of pure graphite persist from (at least) stage 9 to stage 4 in acceptor-intercalated samples, and to stage 3 in donor samples. The absence of a Burstein-Moss shift is interpreted to mean that the partially ionized intercalant layers are screened by the compensating free carriers within one layer spacing, in agreement with a recent calculation. This in turn means that the Madelung energy has a negligible effect in stabilizing the ordered c -axis superlattice observed in dilute compounds.

One of the more striking features of graphite intercalation compounds is the existence of well-ordered \bar{c} -axis superlattices corresponding to separations between intercalant (I) monolayers as large as 30 \AA .¹ The I layers are invariably ionized to some extent, and will therefore be screened by the compensating free charge which resides principally on the intervening carbon (C) monolayers. The compensating charge is delocalized parallel to the layers, giving rise to the well-known enhancement in basal plane conductivity σ_a .

This paper deals with the question of interlayer, or \bar{c} -axis localization (or screening), which is of interest for several reasons. First, the extent of \bar{c} -axis screening determines the relative contributions of different C layers to various properties. For example, if the effective screening length Λ were ~ 1 interlayer spacing, the repeat unit for a dilute compound could be modeled as $I-C_b-C_i \cdots C_i-C_b-I$, where the bounding layers C_b contain most of the delocalized excess charge and the interior layers C_i are essentially identical to the layers in pure graphite. Screening this strong would clearly require modification of the rigid-band approach.² Second, since a C_b-I-C_b unit would be electrically neutral, one would no longer be able to invoke electrostatic repulsion to explain the existence of well-ordered high-stage compounds.

Several authors have discussed this problem recently. Spain and Nagel estimated $\Lambda(\text{max}) \sim 5 \text{ \AA}$ using the Fermi wave vector of pure graphite.³ Solin deduced from Raman data that the charge density is greater on C_b layers than on C_i layers.⁴ Batallan *et al.* found identical magnetothermal oscillation frequencies in stage 2 and stage 4 acceptor compounds, indicating that the two-dimensional (2-D) metallic behavior arises from identical C_b-I-C_b units regardless of their separation.⁵ Pietronero *et al.*^{6,7} calculated the nonlinear screening as a function of total charge density (i.e., fractional ionization of the I layers), and found that for reasonable parameter

values ρ falls by an order of magnitude between C_b and its neighboring C_i . These results all suggest that the screening is indeed short range.

The present work reinforces the above observations by demonstrating an immeasurably small Burstein-Moss shift of graphite interband transitions in dilute compounds. The optical data are supported by x-ray diffractograms which establish the existence of well-ordered c -axis superlattices with repeat distances exceeding the "effective Λ " by at least a factor of 10. We conclude that the Fermi energy in the C_i layers is shifted by less than a few kT ($\sim 0.05 \text{ eV}$).

One type of experiment consisted of alternately measuring (001) x-ray diffractograms and reflectivity spectra *in situ* during intercalation of highly oriented pyrolytic graphite (HOPG) with HNO_3 , AsF_5 , Br_2 , etc. We present here the HNO_3 results. Adding ~ 3 atm argon to the 24°C vapor pressure of HNO_3 , and starting with a sample 0.2 mm thick along \bar{c} , allowed us in effect to take snapshots of metastable stoichiometries (i.e., high stages) as the system approached equilibrium (in this case stage 2). Without the Ar diluent, the surface immediately went to stage 2 with the interior remaining graphite; in particular, intermediate stages were not observed, at least not as pure phases.⁸ Diffractograms (θ - 2θ scans) were obtained with Mo $K\alpha$ radiation, an intrinsic Ge detector at 77 K, and a single-channel analyzer operating at an energy resolution of 2%. The low-index region (small 2θ) is crucial, because it emphasizes the surface and provides the most direct discrimination between stages n and $n \pm 1$.

Reflectivity (R) spectra were measured relative to a gold reference mirror and then differentiated numerically using a mesh of 0.01 eV per point (the same as the interval between R measurements). Use of the log derivative $d \ln R / dE$ eliminated uncertainties in absolute intensity measurement. A five-point smoothing was incorporated into the derivative program, so the first and last two data points of a given 100-point derivative spectrum are not significant.

Figure 1 shows the low-angle portions of several diffractograms measured at times ranging from 0 to 90 hours after starting the reaction. The topmost pattern is for pure graphite. The second diffractogram is interpreted as stage 9 (34.58-Å repeat distance), because the separation between the small peaks at 10.55° and 14.25° fits stage 9 better than stage 8 or 10. The third diffractogram, taken with higher gain, exhibits several peaks which fit stage 8, plus a background that follows the expected variation

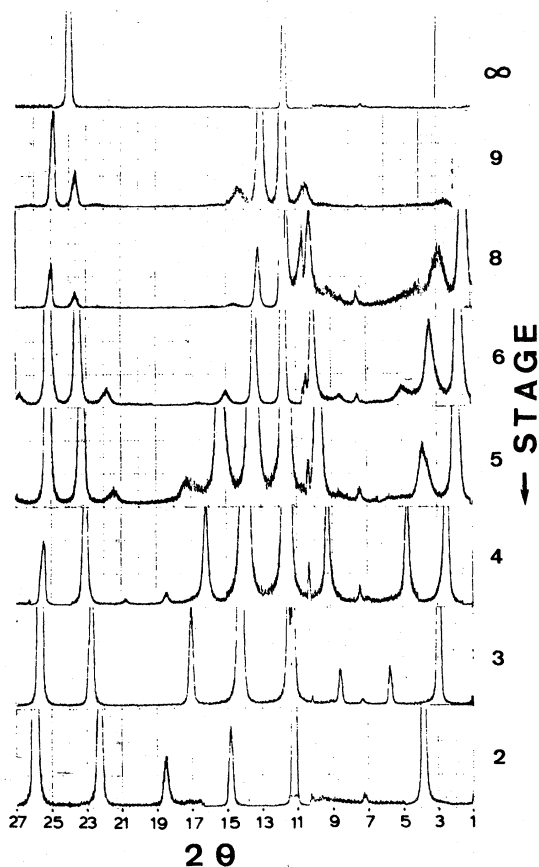


FIG. 1. Evolution of stages during HNO_3 intercalation, observed via (001) x-ray diffraction. The first diffractogram is for pure graphite (stage ∞). The second was taken with insufficient gain to see peaks with $l < 9$, so the assignment of stage 9 is based only on 2θ differences. The third, identified as stage 8, shows the strong (001) reflection at $2\theta = 1.3^\circ$ (expected value 1.5°). The shift of the (001) peak to larger 2θ values is a good signature of the progression of stages. We missed pure stage 7 due to experimenter fatigue. Artifacts from the sample holder occur at 7.4° – 7.6° and 10.2° – 10.4° and are more or less visible in all diffractograms depending on the gain used. A cumulative zero shift due to sample expansion was corrected from time to time but *not* before each scan. With both sample and acid at 24°C , the maximum concentration is stage 2, so only the last diffractogram represents an equilibrium compound.

in Bragg intensity versus 2θ . As the system approaches equilibrium (i.e., as the stage number decreases), the 0 – 10° region becomes cleaner and the assignment of a unique, well-defined stage becomes more certain. The poor quality of the high-stage diffractograms may be partially due to the metastability of these phases under the experimental conditions employed.^{8,9} This is not a crucial issue for interpreting the optical data, however, since the important spectral changes occur after stage 4.

Figure 2 shows $d \ln R / dE$ spectra of HNO_3 compounds corresponding to the stages presented in Fig. 1. The initial curve for pure graphite is featureless at the sensitivity employed. As intercalation begins, three resonant structures appear. The lowest energy structure has a zero crossing at 0.55 eV, corresponding to the dip in reflectivity reported by Fischer *et al.*^{10,11} and by Hanlon *et al.*¹² in various acceptor-type compounds. The other two, which are initially

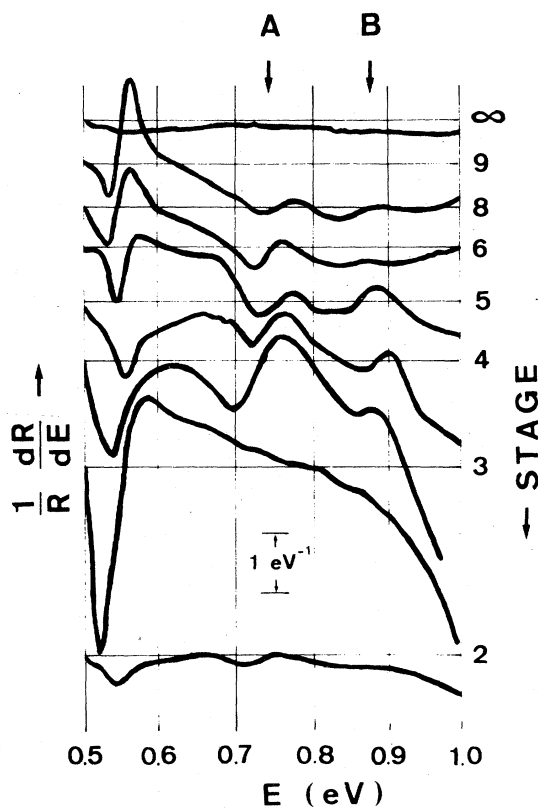


FIG. 2. Progression of $d \ln R / dE$ spectra during HNO_3 intercalation as the sample passes from stage ∞ (i.e., graphite) to stage 2, corresponding to the diffractograms of Fig. 1. Similar data are obtained with other intercalants (see text). The transitions labeled A and B are characteristic of pure graphite and are sensitive to E_F (Ref. 13 and Fig. 4). The absence of Burstein-Moss shifts for $\infty < n < 4$ indicates that the intercalant layers are screened by the free carriers within one layer spacing.

weaker than the 0.55-eV structure, are labeled *A* and *B* since we will identify them as the similarly labeled interband transitions in pure graphite.¹³ In addition, the background above 0.7 eV becomes negative, signaling the emergence of a plasma edge which moves to higher energy with increasing concentration.¹⁰⁻¹² The 0.55-eV structure grows to a maximum at stage 3, then abruptly decreases in magnitude at stage 2. The 0.75-eV transition (*A*) also grows, reaches a maximum at stage 4, then disappears at stage 3. The 0.86-eV transition (*B*) behaves similarly, but is strongly masked at stage 4 by the plasma edge response which has a peak amplitude of $\sim 20 \text{ eV}^{-1}$ at 1.1 eV. None of the three structures shift significantly, variations in line shape being due to concurrent changes in the background reflectivity (see below). This experiment was repeated three times, and the general behavior described above was reproducible.

An identical (*in situ*) experiment was performed with AsF_5 , another electron acceptor. In contrast to HNO_3 diluted with Ar, stage 4 was the most dilute pure phase obtained. The same three structures were observed, the only difference being that the 0.55-eV peak reached maximum strength at stage 4 rather than stage 3. (This is also evident in the raw data of Hanlon *et al.*¹²)

In the case of bromine, we were unable to obtain metastable pure stages more dilute than the saturation value stage 2, despite the addition of $\sim 5 \text{ atm}$ Ar. Wachnik¹⁴ has measured reflectivity spectra from high-stage Br-graphite by preparing various equilibrium samples, and he also observed the 0.55-eV dip in addition to the metallic edge. The *A* and *B* peaks were not resolved in his experiment.

Corresponding spectra were obtained on alkali-metal compounds in a second series of experiments. Here the shift in E_F is expected to be in the opposite direction compared to HNO_3 , because alkali metals act as electron donors while acids, halogens, etc., are acceptors.¹⁵ Figure 3 shows the results for potassium stages 2, 3, 4, 7, and 8. The stage 2 sample was sealed off in the ampoule in which it was prepared, while the higher stage samples were cleaved from thicker specimens and transferred to small pyrex ampoules in a glove box. X-ray analyses were performed on all samples, and in all cases the (001) patterns could be interpreted as pure phases. The general features are similar to the HNO_3 data of Fig. 2. The major structure is again the 0.55-eV transition, although its intensity variation with stage is distinctly different than in HNO_3 compounds (Fig. 2). A new feature is the small structure at 0.63 eV, whose intensity variation with stage qualitatively follows that of the 0.55-eV peak. The *A* and *B* peaks are again observed, but now disappear at stage 2 rather than at stage 3 (HNO_3 , Fig. 2). At stage 1, no structure other than the plasma edge¹⁶ is observed.

The most striking aspect of the spectra in Figs. 2

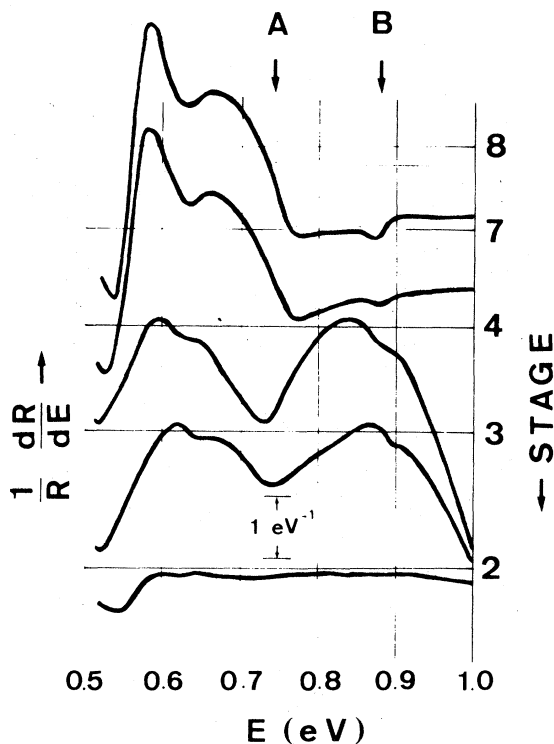


FIG. 3. Similar to Fig. 2 for the donor intercalant potassium. These spectra were obtained from individual samples prepared by equilibrium methods.

and 3 is that the positions of the four structures observed are independent of stage and intercalant species. Variations in amplitude are more difficult to discuss, since they can be attributed either to variations in the strength of the critical-point contribution or to changes in the background dielectric constant, as discussed below.

The principal results we wish to discuss are the existence and constant position of *A* and *B*. We associate these with *K* point interband transitions of pure graphite,¹³ the transition energies being defined essentially by a nearest-layer overlap γ_1 .¹⁷ The fact that they persist to stage 4 (or 3) and disappear at stage 3 (or 2) is consistent with the sandwich model described above: the minimum condition for defining a graphitelike γ_1 is $I-C_b-C_i-C_i-C_b-I$, where the C_i-C_i core gives rise to the graphite transitions. The C_b-C_i interactions are still important, however, because the difference between the two transition energies is defined by second-layer coupling.¹⁷

Of greater significance is the absence of Burstein-Moss shifts of *A* and *B* within the graphitelike core.¹⁸ The *A* and *B* transitions have been identified in pure graphite as shown in Fig. 4(a). Here we draw E_F with a finite width and set the graphite band parameters Δ and γ_2 equal to zero to emphasize the conse-

quences of a room-temperature experiment ($kT \geq \Delta$, γ_2). Under the assumptions² of rigid bands and uniform charge transfer to all C_i layers (i.e., $\Lambda = \infty$), one would expect characteristic Burstein shifts of A (0.74 eV) or B (0.88 eV) according as one intercalates with a donor or acceptor respectively. These are shown schematically in Figs. 4(b) and 4(c). The shift of E_F for a given stage depends on the overall charge transfer; recent experiments¹⁹ and calculations²⁰ indicate that ΔE_F is ~ 1 eV at stage 1, and so is almost certainly less for the concentrations of interest here. If Λ were greater than one interlayer spacing, acceptor intercalation would eventually cause B to blueshift without limit while A would do nothing at 300 K. For donors the opposite holds; A should redshift, B should do nothing. From the data of Figs. 2 and 3 we conclude that neither A nor B shift by more than 0.03 eV. For acceptors (Fig. 2),

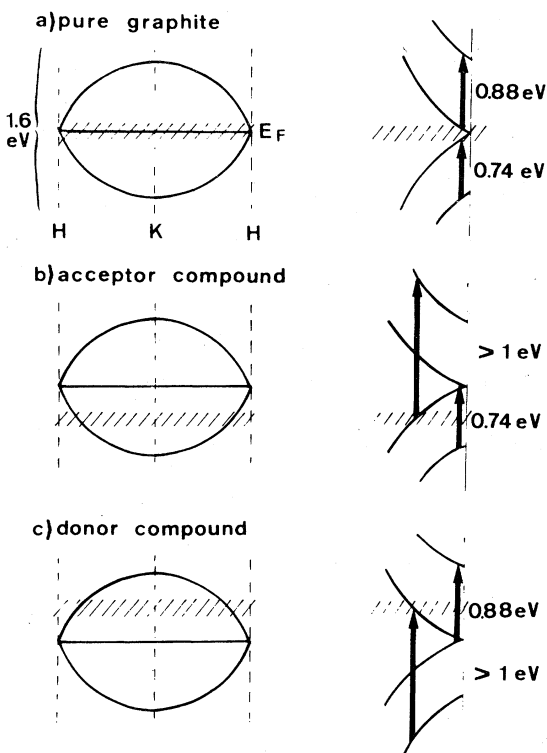


FIG. 4. Interband transitions in pure graphite (Ref. 13) and their expected Burstein shifts with intercalation (Ref. 18), based on the assumptions of rigid bands and uniform c -axis charge distribution. Drawn schematically for $T = 300$ K; the "width" of E_F is exaggerated. (a) Pure graphite, both transitions involve E_F as either initial or final state. (b) Acceptor compound, E_F decreases: the A transition (0.7 eV) remains unchanged, but B should blueshift continuously. (c) Donor compound, E_F increases: B remains unchanged and A blueshifts. The data of Figs. 2 and 3 do not agree with this picture; we conclude that the c -axis charge distribution is highly nonuniform.

the transition expected to move is the upper one (B) so one might lose it due to interference with the plasma edge. This possible ambiguity does not exist for donors (Fig. 3), since A is the one which should shift and it is well away from the plasma edge.

The rigid-band model² can be used to estimate the shift expected in the extreme case $\Lambda = \infty$; taking 0.2 as the fractional ionization of HNO_3 ,²¹ one would expect shifts of 0.3 eV at stage 8, > 0.5 eV at stage 4. This is clearly inconsistent with the data. Taking $\Delta E_F = 0.05$ eV as a generous upper limit and using Ref. 6, we find that the effective Λ (defined as the distance in which ρ falls to $1/e$ its value at a C_b layer) is ~ 1 layer spacing. Thus the results presented here confirm previous suggestions,³ calculations,⁶ and indirect observations^{4,5} that the intercalated ionic layer is strongly screened within one layer. Put another way, the excess free carriers induced by intercalation are largely confined to the neighboring graphite layers (i.e., the C_b layers).

It is difficult if not impossible to deduce a quantitative c -axis charge distribution from our data. Indeed it is somewhat surprising that both the present experiment and the quantum oscillation study⁵ imply a sharp demarcation between C_b and C_i layers, the latter containing essentially no excess charge. This is in contrast to the continuous distribution calculated by Pietronero *et al.*,⁶ according to which one should observe an average Burstein shift or extremal Fermi surface (and broad responses) corresponding to a near-exponential variation in E_F from layer to layer.

We turn now to the significance of the amplitudes of A and B versus stage. The small-signal equation of modulation spectroscopy²² is

$$\frac{\Delta R}{R} = \alpha(\epsilon_1, \epsilon_2) \Delta \epsilon_1 + \beta(\epsilon_1, \epsilon_2) \Delta \epsilon_2,$$

where α and β include all contributions to the dielectric response whereas $\Delta \epsilon_1$ and $\Delta \epsilon_2$ are presumed to come only from the critical points. In principle, variations in $\Delta R/R$ (either in amplitude or in line shape) versus intercalant concentration can be due to variations of either the critical-point contribution or the noncritical background as represented by α and β . In the present experiment we are faced with the problem of separating the stage dependence of the magnitudes of A and B (a $\Delta \epsilon$ effect) from the drastic changes in overall dielectric behavior: from graphite, a semimetal with interband transitions extending to very low frequencies, to nearly classic metallic behavior (an α, β effect).

The first question is: if A and B are graphite transitions, why do we not see them at "stage ∞ " (Fig. 2)? They are typically observed in thermoreflectance spectra¹³ with an amplitude $|\Delta R/R| \sim 10^{-4}$, which would correspond to a log derivative amplitude (0.01-eV energy mesh) of 10^{-2} eV^{-1} , two decades

smaller than the gain marker on Fig. 2. Second, what is the significance of their emergence at stage 9 and apparent growth up to stage 4 (Fig. 2)? For pure graphite in the spectral range of interest²³ $\epsilon = 6 + i10$, from which $\alpha = -0.047$, $\beta = +0.043$. The optical constants of the compounds are not known, but we can estimate α and β from the Drude model. Taking $\omega = \frac{1}{2}\omega_p$, $\omega_p\tau = 50$ we find $\alpha = 0$, $\beta = -0.5$. Thus, with no changes in the fundamental quantity $\Delta\epsilon$, we expect $\Delta R/R$ to increase in amplitude by roughly a factor 10 in accordance with the data. Furthermore, the small apparent peak shifts in Fig. 2 can be attributed to a varying admixture of $\Delta\epsilon_1$ and $\Delta\epsilon_2$ line shapes; for graphite $\Delta R/R(\omega) \sim -\Delta\epsilon_1(\omega) + \Delta\epsilon_2(\omega)$ whereas for a metallic compound $\Delta R/R(\omega) \sim -\Delta\epsilon_2(\omega)$. We conclude from the above that the only significant feature of the intensity variations of *A* and *B* with stage is their disappearance at stage 3 (HNO₃) or stage 2 (K). Furthermore, the apparent small redshift of *A* with decreasing stage for both acceptor and donor series is most likely an effect of varying $\Delta\epsilon_1$, $\Delta\epsilon_2$ admixture.

The identification of the two low-energy transitions at 0.55 and 0.63 eV remains an open question. Several possibilities were considered and rejected: (i) In the first paper on HNO₃-graphite¹¹ we speculated that the 0.55-eV dip in *R* might be due to O-H stretching vibration within the HNO₃ molecule, by analogy to the strong absorptions at 0.42 and 0.84 eV in H₂O. This is clearly wrong since the transition also occurs in compounds with no intramolecular modes (e.g., potassium). (ii) Holzwarth pointed out to us²⁴ that the *K*-point bandwidth for *n* graphite layers increases rather slowly with *n*, starting at zero for *n* = 1. Thus the lower pair of transitions might be ascribed to "local modes" of *n* C_{*i*} layers superposed on the *A* and *B* transitions appropriate to an infinite system. This also fails because the low-energy transitions do not shift with *n*. (iii) The 0.55-eV peak might be ascribed to a charge-transfer transition, as in molecular crystals, whereby an electron is excited from *E_F* in a C_{*b*} layer to an empty state in a C_{*i*} layer. In this case the transition energy would be a measure of the difference in electronic energy between C_{*b*} and C_{*i*}, and would thus depend on the details of the screening as well as on the amount of charge transferred. The latter quantity almost certainly varies to some extent with intercalant species,¹⁵ so one is again at a loss to explain the universal value of the transition energy.

At this point all we can do is speculate that the two low-energy transitions are associated with the existence of "isolated" C_{*b*} layers (i.e., *I*-C_{*b*}-C_{*i*} units) since they essentially disappear when nearest-

neighbor C_{*b*}'s are not separated by at least one C_{*i*}. It is probably significant that the 0.55-eV transition disappears more gradually for donors (Fig. 3) than acceptors (Fig. 2), since many other experiments^{1,15} imply greater interlayer coupling in the former. A comparison of σ_c versus stage between donors and acceptors might help solve this problem.

In summary, the persistence of graphitic *A* and *B* transitions at their unshifted values leads us to conclude that very little if any charge is transferred to the C_{*i*} layers. A generous upper limit for ΔE_F in the C_{*i*} layers, is 0.05 eV. If one insists on defining a screening length as the $1/e$ decay length, then it must be less than a layer spacing. This conclusion has some important implications. The short screening length indicates that the in-plane metallic character is due to C_{*b*}-*I*-C_{*b*} units.⁵ The maximum σ_a is typically at stage 3 or 4,¹⁵ which is where one would expect overlap between units to set in. The stage dependence of σ_c should also be sensitive to screening, especially in donor compounds for which the *c*-axis conductance of a C_{*b*}-*I*-C_{*b*} unit is large. Here the screening would reduce σ_c of high-stage compounds relative to what would be expected with a uniform charge density.

The most puzzling consequence of the screening result is, since a C_{*b*}-*I*-C_{*b*} unit is essentially neutral, one can no longer invoke electrostatic repulsion to explain the stability of high-stage superlattices. The elastic energy is not a likely candidate either, since the interlayer separation is independent of period (i.e., the length C_{*i*}-C_{*i*} is independent of stage and equal to the length C_{*b*}-C_{*i*}). Young²⁵ has proposed a charge-density wave mechanism in this context, which also explains some features of the intercalation reaction.

Finally, we note that the Landau level study of dilute graphite-bromine²⁶ may have been sensitive only to C_{*i*} layers, in which case the estimate of 2% ionization of the Br₂ molecules would be far too low.

ACKNOWLEDGMENTS

We acknowledge the experimental assistance of M. J. Moran, R. Grayeski, and L. R. Hanlon. C. Underhill of M.I.T. provided invaluable counsel regarding x-ray equipment. The HOPG was kindly furnished by A. W. Moore, of Union Carbide. This research was supported mainly by ONR Contract No. N00014-75C-0751; we also acknowledge use of the LRSM Central Facilities supported by the NSF Materials Research Laboratory Program, Grant. No. DMR-76-80994.

- ¹For a recent summary of the field, see *Mater. Sci. Eng.* **31** (1977).
- ²M. S. Dresselhaus, G. Dresselhaus, and J. E. Fischer, *Phys. Rev. B* **15**, 3180 (1977).
- ³I. L. Spain and D. J. Nagel, *Mater. Sci. Eng.* **31**, 183 (1977).
- ⁴S. A. Solin, *Mater. Sci. Eng.* **31**, 153 (1977).
- ⁵F. Batallan, J. Bok, I. Rosenman, and J. Melin, *Phys. Rev. Lett.* **41**, 330 (1978).
- ⁶L. Pietronero, S. Strässler, H. R. Zeller, and M. J. Rice, *Phys. Rev. Lett.* **41**, 763 (1978). The value of ϵ_{11} used by these authors is too large [M. Zanini, D. Grubisic, and J. E. Fischer, *Phys. Status Solidi B* **90**, 151 (1978)], which means the theoretical "A" is even smaller.
- ⁷L. Pietronero, S. Strässler, and H. R. Zeller, *Solid State Commun.* **30**, 399 (1979).
- ⁸The usual method of synthesizing a desired stage involves controlling the vapor pressure of the intercalant over the compound, i.e., controlling separately $T(\text{compound})$ and $T(\text{intercalant})$. This equilibrium approach would have been difficult to incorporate into our experiment. We are in essence exploiting the phenomenon of "spontaneous staging" discussed by Falardeau *et al.*, *Inorg. Chem.* **17**, 301 (1978).
- ⁹H. Fuzellier, thesis (University of Nancy, France, 1974) (unpublished).
- ¹⁰J. E. Fischer, T. E. Thompson, G. M. T. Foley, M. Hoke, and F. L. Lederman, *Phys. Rev. Lett.* **37**, 769 (1977). In this work and in the following reference, the sample surfaces were briefly exposed to air, and the 0.55-eV structure appeared to blueshift with increasing concentration. The present data imply that this shift was attributable in some way to the air exposure.
- ¹¹J. E. Fischer, T. E. Thompson, and F. L. Vogel, in *Petroleum-Derived Carbons*, edited by M. L. Deviney and T. M. O'Grady, ACS Symposium Series No. 21 (American Chemical Society, Washington, D.C., 1975), p. 418.
- ¹²L. R. Hanlon, E. R. Falardeau, and J. E. Fischer, *Solid State Commun.* **24**, 377 (1977); also L. R. Hanlon *et al.*, *Mater. Sci. Eng.* **31**, 161 (1977).
- ¹³G. Bellodi, A. Borghesi, G. Guizzetti, L. Nosenzo, E. Reguzonni, and G. Samoggia, *Phys. Rev. B* **12**, 5951 (1975).
- ¹⁴R. A. Wachnik, B. S. thesis (M.I.T., 1977) (unpublished).
- ¹⁵Recent data summarized by J. E. Fischer and T. E. Thompson, *Phys. Today* **31**, No. 7, 36 (1978).
- ¹⁶D. Guerard, G. M. T. Foley, M. Zanini, and J. E. Fischer, *Nuovo Cimento B* **38**, 410 (1977).
- ¹⁷J. W. McClure, in *Semimetals and Narrow-Gap Semiconductors*, edited by D. L. Carter and R. T. Bate (Pergamon, New York, 1971), p. 127.
- ¹⁸G. Dresselhaus and M. S. Dresselhaus, *Mater. Sci. Eng.* **31**, 235 (1977).
- ¹⁹B. R. Weinberger, J. Kaufer, A. J. Heeger, J. E. Fischer, M. J. Moran, and N. A. W. Holzwarth, *Phys. Rev. Lett.* **41**, 1417 (1978).
- ²⁰N. A. W. Holzwarth, S. Rabii, and L. A. Girifalco, *Phys. Rev. B* **18**, 5190 (1978).
- ²¹S. Loughin, R. Grayeski, and J. E. Fischer, *J. Chem. Phys.* **69**, 3740 (1978).
- ²²J. E. Fischer and D. E. Aspnes, *Comments Solid State Phys.* **4**, 131 (1972).
- ²³E. A. Taft and H. R. Philipp, *Phys. Rev. A* **138**, 197 (1965).
- ²⁴N. A. W. Holzwarth (private communication).
- ²⁵D. A. Young, *Carbon* **15**, 373 (1977).
- ²⁶D. A. Platts, D. D. L. Chung, and M. S. Dresselhaus, *Phys. Rev. B* **15**, 1087 (1977).